Maximum Torque per Ampere (MTPA) Control of an IPM Machine Based on Signal Injection Considering Inductance Saturation

Sungmin Kim, *Student Member, IEEE*, Young-Doo Yoon, *Member, IEEE*, Seung-Ki Sul, *Fellow, IEEE*, and Kozo Ide, *Member, IEEE*

***Abstract*—The aim of this study was to develop a new method to operate an interior permanent magnet synchronous machine (IPMSM) on the maximum torque per ampere (MTPA) condition. The characteristics of the MTPA condition were analyzed and the MTPA condition was derived based on the input electric power. The proposed method injects a small current signal used for tracking the MTPA operating point along with the fundamental current for torque generation. This method does not require any machine parameters or premade lookup table. The frequency of the injected signal is several hundred hertz, and the performance of the MTPA tracking is almost free from load torque disturbance. The feasibility of the proposed method was verified under various operating conditions with computer simulation and testing with an 11 kW IPMSM drive system.**

***Index Terms*—Efficiency operation, interior permanent magnet synchronous machine (IPMSM), maximum torque per ampere (MTPA), signal injection.**

I. Introduction

ELECTRIC machines, which convert electric energy into mechanical energy, are the largest consumers of electric power. A variety of energy issues have emerged in the world and in response there have been a wide variety of studies aimed at increasing the efficiency of electric machines from every aspect in industrial applications. When compared with an induction machine, the most popular machine in industrial applications, a permanent magnet synchronous machine (PMSM), is an attractive alternative ac machine due to its higher power density, higher torque density, and higher efficiency. Recently, the use of PMSMs in general industrial fields have become more popular, and as a result the design and control methodology of PMSMs have been intensively researched for the last several decades [1].

Manuscript received October 25, 2011; revised December 12, 2011, January 17, 2012, and February 29, 2012; accepted April 2, 2012. Date of current version September 11, 2012. This paper was presented in part at the Applied Power Electronics Conference and Exposition, Palm Springs, CA, February 21–25, 2010. Recommended for publication by Associate Editor K. M. Ralph.

S. Kim and S.-K. Sul are with the School of Electrical Engineering and Computer Science, Seoul National University, Seoul 151-742, Korea (e-mail: ksmin@eepel.snu.ac.kr; sulsk@plaza.snu.ac.kr).

Y.-D. Yoon is with Samsung Electronics, Suwon 442-742, Korea (e-mail: youngdoo.yoon@gmail.com).

K. Ide is with Yaskawa Electric Corporation, Kitakyushu 806-0004, Japan (e-mail: kozo@yaskawa.co.jp).

Color versions of one or more of the figures in this paper are available online at http://ieeexplore.ieee.org.

Digital Object Identifier 10.1109/TPEL.2012.2195203

Among the PMSMs, the interior permanent magnet synchronous machine (IPMSM), which has a permanent magnet inside of the rotor, has replaced the induction machine in several industrial applications. The rotor structure of the IPMSM leads to mechanical robustness under high-speed operating conditions and features under flux-weakening operations [2]. Compared to a surface permanent magnet synchronous machine (SPMSM), the distinct characteristic of an IPMSM is its inductance saliency, i.e., the d-axis inductance is different from the q-axis inductance. Since the permanent magnets of an IPMSM are buried inside the rotor at the d-axis, the q-axis inductance in the synchronous reference frame is conspicuously larger than the d-axis inductance. This difference between the q-axis and d-axis inductances contributes to the additional torque that is generated, called the reluctance torque. Therefore, the generated torque in an IPMSM consists of the field torque from the permanent magnet and the reluctance torque. The former is proportional to the q-axis current, and the latter is related to multiplication of the d-axis current with the q-axis current. With a constant magnitude of currents, the torque of an IPMSM can be generated differentially according to the angle of the stator current vector. Among the various current vectors that generate a specific torque, the current vector, which has a minimum magnitude of the current vector, is called the maximum torque per ampere (MTPA) current. Additionally, the MTPA can also be considered as the current vector that generates the maximum torque with a constant magnitude. Since IPMSM has no rotor copper loss, the MTPA operation guarantees minimum copper loss of the IPMSM under the given operating conditions. Furthermore, in general, the iron loss of the IPMSM below the speed of the flux-weakening region is negligible compared to the copper loss and it is little affected by the angle variation of the stator current vector. Therefore, the MTPA operation, which means the minimum copper loss, can be understood as the operating condition at maximum efficiency.

Many studies have been done on the control of IPMSMs with MTPA operations. Those results are divided into three groups: 1) MTPA point calculation based on machine parameters; 2) minimum current operation using the searching algorithm; and 3) MTPA point tracking with an additional signal injection. First, the MTPA point can be found with mathematical calculations using the machine model. At its inception, the calculations were achieved with nominal machine parameters [3], [4]. However, the parameters of an IPMSM vary extremely for a variety of reasons including stator currents, temperature, rotating speed

of the machine, and so on [5]. Moreover, the q-axis inductance significantly changes based on the stator current vector. That means the flux is saturated due to the stator current. Therefore, these MTPA points from the calculations based on the machine model are vulnerable to variations in the parameters regardless of the enormous effort to compensate for parameter variation using online estimation techniques [6]–[9] or premade lookup tables [10]–[12]. Moreover, the MTPA points have been tested in an offline system, and the current reference vectors from the test results have been used in real operations [13], [14].

Second, the MTPA points can be detected with a searching algorithm [15], [16]. By changing the current vector, the minimum magnitude of the current vector can be searched for in the constant load torque condition. These methods can find the MTPA point without any parameters. However, the stability of the searching algorithm itself cannot be guaranteed under varying load torque conditions and the searching algorithm is very slow.

Finally, the MTPA points can be detected instantaneously with the injection of high-frequency current [17]–[19]. These methods basically depend on the characteristic of the MTPA points which is that the variation in the torque based on the variation in the current angle is zero at the MTPA points. Based on this characteristic, the MTPA points can be detected from the response in the torque by injecting a high-frequency current signal. In a real system, however, it is very difficult to instantaneously obtain the value for the variation in the torque. In a previous study [18], the variation in the speed due to the injected current signal was used instead of the variation in the torque. However, the performance of this method was limited due to the resolution of the position/speed sensor. In the experiment in [18], the frequency of the injected current signal was very low, and the tracking performance was not reasonable in varying load and/or varying speed conditions. In addition, the speed ripple at the injection frequency exited for the MTPA operation. In a previous study [20], mechanical power was substituted for the torque. Since the mechanical power could be calculated from the stator voltage and current, the frequency of the injected current signal was only limited by the current control bandwidth. Therefore, several hundred hertz signal was injected to detect the MTPA points and the MTPA point was tracked in real time.

This study extends the MTPA point tracking method in [20] and [21] and provides analysis using the varying inductance model of IPMSMs. Due to the relatively high frequency of the injected current signal, the proposed method shows robustness under varying load and speed conditions. A supplementary high-frequency current control loop is used to inject the high-frequency current signal. From the simulation and experimental results, the feasibility of the proposed method was verified.

II. IPMSM Characteristics and MTPA Operation

From the equivalent models in Fig. 1, the voltage equations of the IPMSM are obtained as follows:

$$\begin{aligned} v_{ds}^r &= R_s i_{ds}^r + L_{ds}\frac{di_{ds}^r}{dt} - \omega_r L_{qs} i_{qs}^r \\ v_{qs}^r &= R_s i_{qs}^r + L_{qs}\frac{di_{qs}^r}{dt} + \omega_r \left(L_{ds} i_{ds}^r + \lambda_f\right) \end{aligned} \tag{1}$$

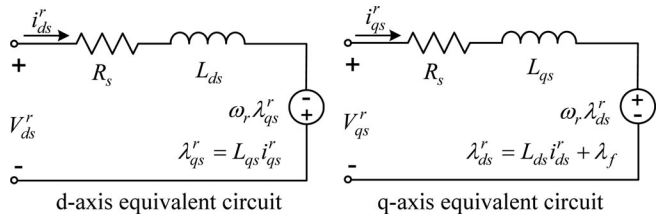

Fig. 1. IPMSM d-/q-axis equivalent model in the synchronous reference frame.

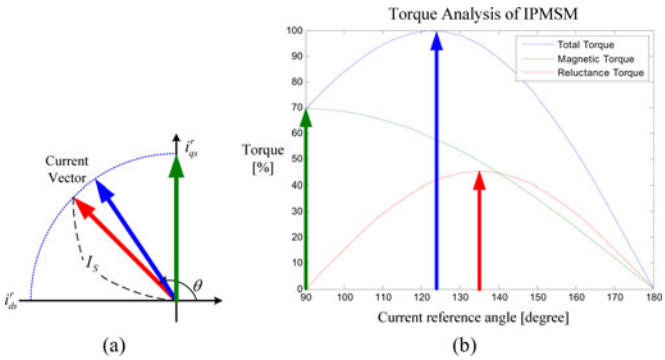

Fig. 2. Current vector and the generated torque of IPMSM. (a) Current vectors in the current plane. (b) Torque analysis of IPMSM.

where v_{ds}^r and v_{qs}^r are the d-/q-axis voltages, i_{ds}^r and i_{qs}^r are the d-/q-axis currents, ω_r is the speed of rotor in the electric angle, and λ_f is a permanent magnet flux linkage. For steady-state operations, the torque that can be generated by IPMSM is calculated as follows:

$$T_e = \frac{3}{2}P\left\{\lambda_f i_{qs}^r + \left(L_{ds} - L_{qs}\right) i_{ds}^r i_{qs}^r\right\} \tag{2}$$

where P is the number of pole pairs. The torque of the IPMSM consists of the field torque from the permanent magnet and the reluctance torque. The field torque is proportional to the q-axis current and the reluctance torque is proportional to the multiplication of the d-axis current with the q-axis current. To analyze the torque and current characteristics, the torque based on the IPMSM model is simulated according to the variation of the current vector with constant magnitude. Fig. 2 shows the simulated torque of the IPMSM and corresponding current vectors. With a constant magnitude of the current vector, the generated torque, shown as a blue line in Fig. 2(b), varies according to the angle of the current vector. The green and red lines in Fig. 2(b) show the field torque and the reluctance torque, respectively. The field torque is maximized with a current vector angle of 90° in Fig. 2(a). On the other hand, the reluctance torque is maximized with a current vector angle of 135°. Therefore, the angle for the maximum torque was between 90° and 135°, and that point is the MTPA point.

The MTPA point is the nearest point to the origin among the points on the constant torque curve in the current plane. And the MTPA is also the current point with a minimum magnitude point in the constant torque curve as shown in Fig. 3. If the variation in the core loss due to the variation in the current vector angle is negligible, the MTPA point is almost the most efficient

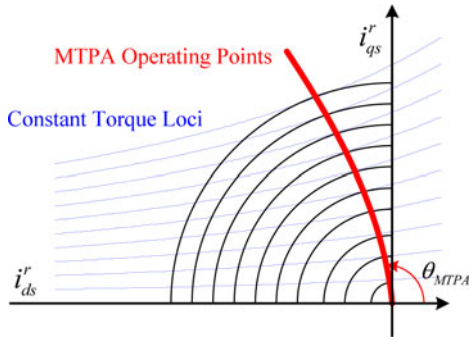

Fig. 3. MTPA operating points and the constant torque loci in the current vector plane.

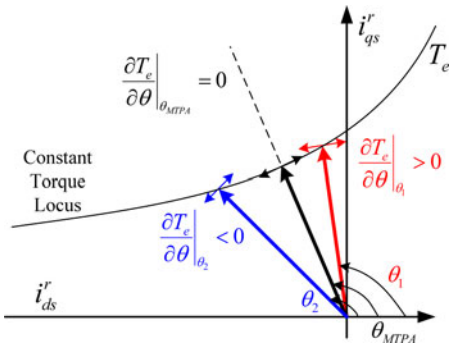

Fig. 4. Locus of the constant torque in the current vector plane.

operating point. In Fig. 3, the MTPA points with constant torque loci are shown in the current plane. The angle of the MTPA current vector varies based on the generated torque. Therefore, the MTPA point can be determined according to the torque condition.

III. Proposed MTPA Tracking Method With Signal Injection

A. Basic Principle

In the synchronous current plane of the IPMSM, there are many current reference pairs $(i^{r*}_{ds}, i^{r*}_{qs})$ that generate a specific torque. To operate the IPMSM in the MTPA condition, the current reference vector should be found for its magnitude to be minimal at a specific torque. In Fig. 4, the constant torque locus is shown in the current plane at the synchronous reference frame. The torque of an IPMSM can be derived as (2). The MTPA operating point is the nearest point to the origin in the current plane. Therefore, the differentiation of the torque with respect to the current angle in the synchronous reference frame, $\partial T_e/\partial\theta$, should be zero at the MTPA point given as follows:

$$\frac{\partial T_e}{\partial \theta} = \frac{3P}{4} I_S \left\{ \lambda_f \cos\theta + (L_{ds} - L_{qs})\, I_S \cos 2\theta \right\} = 0 \quad (3)$$

where I_S is the magnitude of the current, and θ is the angle of the current in the synchronous reference frame shown in Fig. 2(a). From the MTPA criterion equation (3), the current angle of the MTPA point θ_{MTPA} can be derived as

$$\theta_{\mathrm{MTPA}} = \cos^{-1}\left(\frac{-\lambda_f + \sqrt{\lambda_f^2 + 8\,(L_{ds} - L_{qs})^2\, I_S^2}}{4\,(L_{ds} - L_{qs})\, I_S} \right) \quad (4)$$

$$i^r_{ds}\big|_{\mathrm{MTPA}} = I_S \cos\theta_{\mathrm{MTPA}}, \quad i^r_{qs}\big|_{\mathrm{MTPA}} = I_S \sin\theta_{\mathrm{MTPA}}. \quad (5)$$

From (4) and (5), the MTPA operating point can be calculated using the IPMSM parameters. These equations could be derived under the assumptions that the machine inductances and the permanent magnet flux linkage are constant. However, the flux linkage of a permanent magnet varies according to the operating conditions such as rotor temperature and saturation of the machine. Additionally, the *d*-/*q*-axis inductances vary according to the operating conditions. Therefore, (3) should be modified taking into the consideration the variation in the inductances. The criterion of the MTPA point considering the variation in the inductance can be derived as

$$\frac{\partial T_e}{\partial \theta} = \frac{3P}{4} I_s \Bigg\{ \lambda_f \cos\theta + (L_{ds} - L_{qs})\, I_s \cos 2\theta + \left(\frac{\partial L_{ds}}{\partial \theta} - \frac{\partial L_{qs}}{\partial \theta} \right) I_s \frac{1}{2} \sin 2\theta \Bigg\} = 0. \quad (6)$$

If the value of $\partial T_e/\partial\theta$ is evaluated, the control system can recognize whether the present operating point is on the MTPA operating point, even though the torque of the IPMSM is not measured exactly.

B. Evaluation of $\partial T_e/\partial\theta$

Since it is very difficult to calculate or measure the torque in industrial applications, the proposed MTPA tracking method in this paper evaluates the $\partial T_e/\partial\theta$ using the concept of signal injection. The proposed method injects a high frequency, small signal to the current reference angle θ as

$$\theta = \theta_{\mathrm{avg}} + \theta_h = \theta_{\mathrm{avg}} + A_{\mathrm{mag}} \sin(f_h \times 2\pi t) \quad (7)$$

where A_{mag} and f_h are the magnitude and frequency of the injected signal, respectively. The frequency of the injected signal f_h should be high enough compared to the bandwidth of the speed control loop or the torque control loop to prevent interference between the injected signal and the control loops. However, the frequency should be low enough compared to the inverter switching frequency to modulate the injected signal. Additionally, the magnitude of the signal should be small enough not to provoke any variation in speed due to the injected signal.

By injecting the signal to the current angle θ, the control system could experience some variation in mechanical power related to the variation in the torque due to the variation in the current angle. The calculated instantaneous input power from the terminal voltage and current can be used as an index of the variation in the torque. The instantaneous input power includes not only the mechanical power but also the losses due to the stator resistance and the reactive power related to the inductance of the IPMSM. Therefore, to determine the MTPA operating point, the mechanical power from the calculated input

power should be measured. The power due to the injected signal can be analyzed as follows.

From the injected signal, the *d*-/*q*-axis currents can be described as (8) and (9) under the assumption that A_{mag} is much smaller than θ_{avg}

$$\begin{aligned} i_{ds}^{r} &= I_S \cos(\theta_{\mathrm{avg}} + A_{\mathrm{mag}} \sin \omega_h t) \\ &\approx I_S \cos\theta_{\mathrm{avg}} - I_S A_{\mathrm{mag}} \sin\theta_{\mathrm{avg}} \sin\omega_h t \\ &= i_{dsf}^{r} + i_{dsh}^{r} \end{aligned} \tag{8}$$

$$\begin{aligned} i_{qs}^{r} &= I_S \sin(\theta_{\mathrm{avg}} + A_{\mathrm{mag}} \sin \omega_h t) \\ &\approx I_S \sin\theta_{\mathrm{avg}} + I_S A_{\mathrm{mag}} \cos\theta_{\mathrm{avg}} \sin\omega_h t \\ &= i_{qsf}^{r} + i_{qsh}^{r}. \end{aligned} \tag{9}$$

The electric input power can be calculated as (10), which consists of the copper loss, the reactive power, and the mechanical power. Considering the high-frequency current signal, the copper loss P_{copper}, the reactive power P_{reactive}, and the mechanical power P_{mech} can be expressed as (11)–(13), respectively. The copper loss due to the stator resistance is not affected by the injected signal as in (11), since the magnitude of the input current is constant regardless of the injected signal. However, the reactive power and the mechanical power represented by (12) and (13), respectively, contain some variation in the power whose frequency is identical to that of the injected signal. The phase of the injected signal frequency component in the reactive power is out of phase with that of the injected signal itself. For the mechanical power in (13), the phase of the injected signal frequency component is in phase with that of the injected signal and the magnitude of the power variation is proportional to the MTPA criterion in (3)

$$\begin{aligned} P_e &= P_{\mathrm{copper}} + P_{\mathrm{reactive}} + P_{\mathrm{mech}} \\ &= \frac{3}{2}\Bigg\{ R_S \left(i_{ds}^{r2} + i_{qs}^{r2}\right) + L_{ds}\frac{di_{ds}^{r}}{dt} i_{ds}^{r} + L_{qs}\frac{di_{qs}^{r}}{dt} i_{qs}^{r} \\ &\qquad + \omega_r \lambda_f i_{qs}^{r} + \omega_r \left(L_{ds} - L_{qs}\right) i_{ds}^{r} i_{qs}^{r} \Bigg\} \end{aligned} \tag{10}$$

$$P_{\mathrm{copper}} = \frac{3}{2} R_S I_S^2 \tag{11}$$

$$\begin{aligned} P_{\mathrm{reactive}} &\approx -\frac{3}{4}\left(L_{ds} - L_{qs}\right) I_s^2 A_{\mathrm{mag}} \omega_h \sin 2\theta_{\mathrm{avg}} \cos\omega_h t \\ &\quad + \frac{3}{4}(L_{ds}\sin^2\theta_{\mathrm{avg}} + L_{qs}\cos^2\theta_{\mathrm{avg}}) \\ &\quad \times I_S^2 A_{\mathrm{mag}}^2 \omega_h \sin 2\omega_h t \end{aligned} \tag{12}$$

$$\begin{aligned} P_{\mathrm{mech}} &\approx \omega_r \frac{3}{2}\left\{\frac{1}{2}\left(L_{ds} - L_{qs}\right) I_S^2 \sin 2\theta_{\mathrm{avg}} + \lambda_f I_S \sin\theta_{\mathrm{avg}}\right\} \\ &\quad + \frac{3}{2}\{\lambda_f \cos\theta_{\mathrm{avg}} + (L_{ds} - L_{qs}) I_S \cos 2\theta_{\mathrm{avg}}\} \\ &\quad \times I_S \omega_r A_{\mathrm{mag}} \sin\omega_h t \\ &\quad + \frac{3}{8}\omega_r (L_{ds} - L_{qs}) I_S^2 A_{\mathrm{mag}}^2 \sin 2\theta_{\mathrm{avg}} \cos 2\omega_h t. \end{aligned} \tag{13}$$

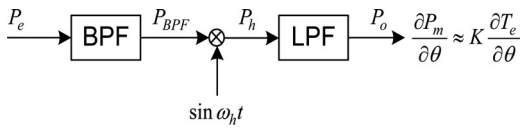

Fig. 5. Signal processing to extract the MTPA criterion.

To evaluate the MTPA criterion, i.e., the differentiation of the torque with respect to the angle of the current vector in the synchronous reference frame $\partial T_e/\partial\theta$, a simple signal processing block can be used as shown in Fig. 5.

To extract the component of the injected frequency f_h from the measured power, the power is processed with a bandpass filter whose center frequency is the injected frequency f_h. Using the bandpass filter, the component of the injected frequency P_{BPF} in the electric input power can be extracted. The result includes not only the component from the mechanical power but also the component from the reactive power. The component from the reactive power is orthogonal to the injected signal seen in (12) and (13). Hence, to extract only the component related to the mechanical power, the output of the bandpass filter can be multiplied with the injected sinusoidal signal. After that, the results should be filtered out by a low-pass filter whose cutoff frequency is far below the injected frequency f_h for filtering out the orthogonal term, which is the component from the reactive power from the results. Through this multiplication operation and low-pass filtering, a component proportional to $\partial T_e/\partial\theta$ can be obtained as P_o described as follows:

$$\begin{aligned} P_0 &= \frac{3}{4}\omega_r A_{\mathrm{mag}} I_S \left\{\lambda_f \cos\theta_{\mathrm{avg}} + \left(L_{ds} - L_{qs}\right) I_S \cos 2\theta_{\mathrm{avg}}\right\} \\ &\propto \frac{\partial T_e}{\partial\theta}. \end{aligned} \tag{14}$$

The criterion in (3), i.e., the differentiation of the torque with respect to the current angle is identical to P_o in (14) except for the proportional constant. Therefore, if the output of the signal processing in Fig. 5 is controlled as null, the MTPA operation is always guaranteed under the assumption of having constant parameters for the IPMSM. If the variation in the inductances due to the magnetic saturation is considered in the proposed method, the result of the signal process P_o can be derived as (15). The MTPA criterion considering the inductance variation in (6) is also identical to P_o in (15) except for the proportional constant. That means the proposed method can track the MTPA point regardless of the variations in the IPMSM parameters. The derivation of (15), which considers the inductance saturation, is given in the Appendix

$$\begin{aligned} P_o &= \frac{1}{2} A_{\mathrm{mag}} \omega_r I_s \Bigg\{\lambda_f \cos\theta + \left(L_{ds} - L_{qs}\right) I_s \cos 2\theta \\ &\qquad + \left(\frac{\partial L_{ds}}{\partial\theta} - \frac{\partial L_{qs}}{\partial\theta}\right) I_s \frac{1}{2}\sin 2\theta \Bigg\}. \end{aligned} \tag{15}$$

Fig. 6 demonstrates the relationship between the angle of the current reference vector, the signals during the signal processing procedure, and the actual torque. The angle of the current reference vector θ is varied from 1.6 to 2.3 rad in Fig. 6(a)

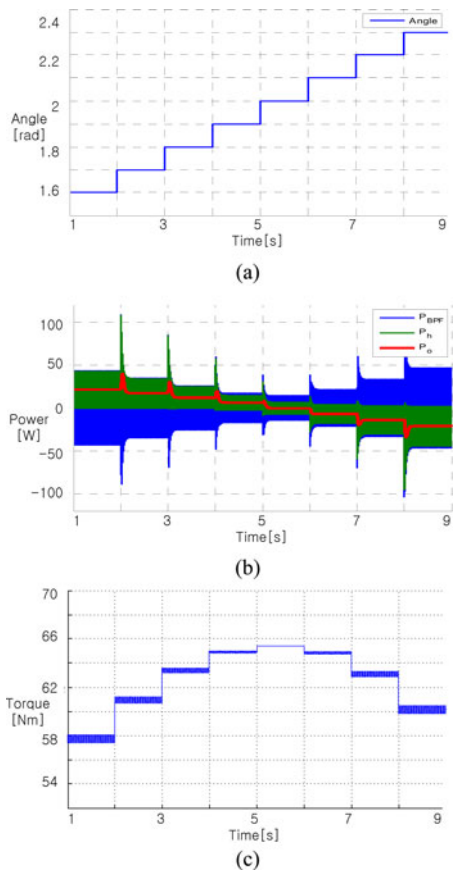

Fig. 6. Simulation result of signal processing. (a) Variation of current reference angle θ. (b) Variation of the signals in the signal processing according to the current reference angle variation in (a). (c) Variation in the torque according to the current reference angle variation in (a).

under the operating conditions of a constant magnitude for the stator current and constant speed. Fig. 6(b) shows the output signal from the bandpass filter P_{BPF}, the signal multiplied by the injected sinusoidal signal P_h, and the output signal P_o of the low-pass filter. Additionally, Fig. 6(c) shows that the torque from the simulation model varied according to the angle of the current reference vector shown in Fig. 6(a). Despite the constant magnitude of the stator current, the torque varied according to the current reference angle. The maximum torque was 66 N·m at $\theta = 2.0$ rad.

As mentioned previously, the output of the signal processing procedure P_o was near zero around the MTPA operating point, 2.0 rad. The resulting P_o of the signal processing was positive whenever the current reference angle was below 2.0 rad. However, P_o was negative whenever the current reference angle was above the angle of the MTPA operating point, 2.0 rad.

C. Understanding the Signal Injection Method

The argument in Sections III-B and III-C can be understood by the Taylor series expansion. The MTPA tracking method using signal injection has its ground in the MTPA definition itself; the variation in the torque according to the variation in the current angle is zero at the MTPA operating point for an IPMSM. To exploit this definition, the variation in the torque has to be detected in the system. Measuring the torque, however, is very difficult and is almost impossible in real industrial applications. The variation in the input electric power can be substituted with the variation in the torque in the proposed method.

Under a constant speed, if the torque varies, the mechanical power varies proportionally to the torque, given by (16). To determine the information on the variation in the torque according to the variation in the current angle, a high-frequency sinusoidal signal is injected into the current reference in the synchronous reference frame. As for the injected signal, the torque can be derived with the Taylor series expansion as

$$P_m = T_e \omega_{rm}, \quad T_e(\theta) = \frac{1}{\omega_{rm}} P_m(\theta) \tag{16}$$

$$T_e(\theta + \Delta\theta) = T_e(\theta) + \frac{\partial T_e}{\partial \theta}\Delta\theta + \frac{\partial}{\partial \theta}\left(\frac{\partial T_e}{\partial \theta}\right)\Delta\theta^2 + \cdots \tag{17}$$

$$T_e(\theta + A\sin\omega_h t) = T_e(\theta) + \frac{\partial T_e}{\partial \theta} A\sin\omega_h t + \frac{\partial}{\partial \theta}\left(\frac{\partial T_e}{\partial \theta}\right) A^2 \sin^2 \omega_h t + \cdots. \tag{18}$$

Since the magnitude of the injected signal is very small and the frequency of the injected signal is high enough compared to the bandwidth for the speed regulation loop, the variation in the speed due to the injected signal can be ignored. The torque would be proportional to the mechanical power as in (16). Additionally, the higher order terms including the second-order terms in (18) can be ignored. From the signal processing, the electric power can be transformed into the variation in the torque according to the variation in the current angle variation as

$$\text{Signal Processing}\{P_e\} \propto \text{Signal Processing}\left\{T_e(\theta) + \frac{\partial T_e}{\partial \theta} A\sin\omega_h t\right\} \propto \frac{\partial T_e}{\partial \theta}. \tag{19}$$

D. Current Signal Injection at High Frequency

Since the proposed method relies on the variation in the input power at the injected signal frequency, the variation in the power should only occur from the injected signal. However, the input power can vary for many reasons such as a change in the speed reference, torque disturbance, load variation, and so on. To separate the power variation due to the injected signal from that due to the other reasons, the frequency of the injected signal should be as high as possible. In this paper, 300 and 350 Hz were used as the frequency of the injected signal. To inject such a high-frequency current signal, a supplementary high-frequency current control loop was augmented into the basic current control loop shown in Fig. 7. The frequency of the injection signal can be selected according to the operating situation to escape resonant issues due to the injected signal. The *d*-/*q*-axis current references were decomposed to the fundamental components i_{dsf}^{r*}, i_{qsf}^{r*} and the high-frequency component i_{dsh}^{r*}, i_{qsh}^{r*} as (8) and (9). As a supplementary high-frequency

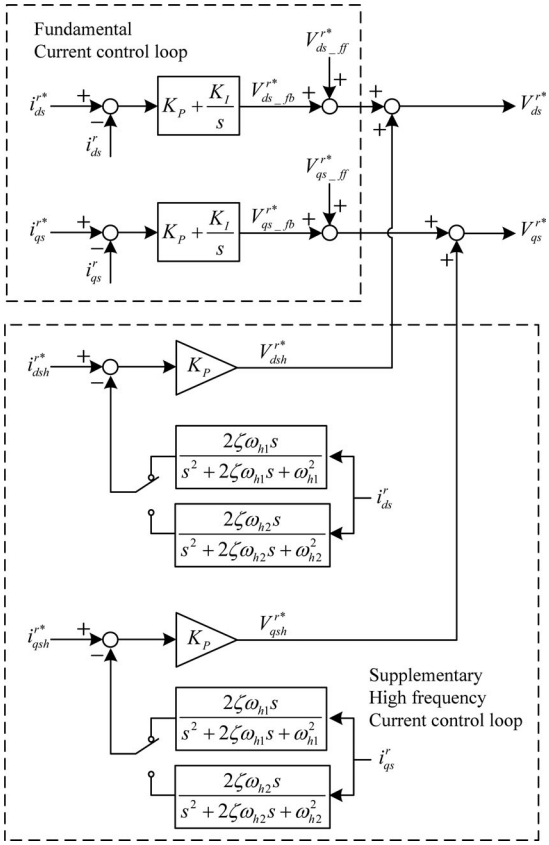

Fig. 7. Current control loop with the supplementary high-frequency current control loop.

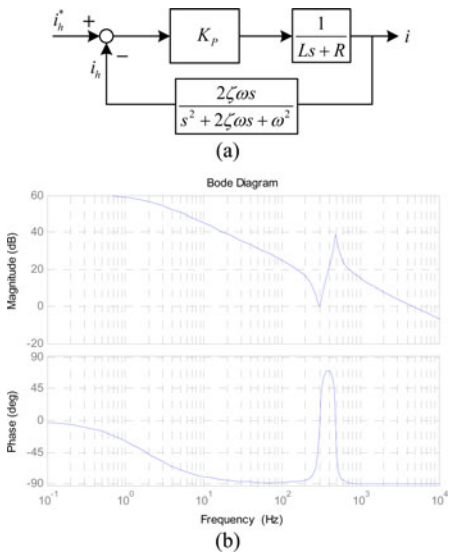

Fig. 8. High-frequency signal P-type control loop. (a) Block diagram of the high-frequency signal control loop. (b) Bode plot of the high-frequency signal control loop.

current control loop, a proportional regulator was incorporated as shown in Fig. 8. The transfer function of the P-type controller can be derived as in (20). The gain of the proportional regulator was set to ten times the impedance of the inductance at the injection frequency, and then, the transfer function can be approximated as unity by

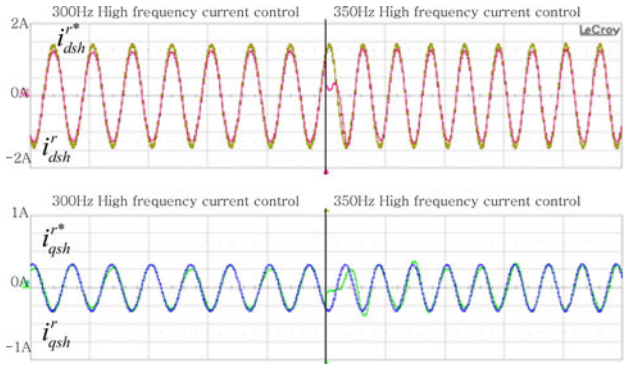

Fig. 9. Performance of the high-frequency *d*-/*q*-axis current control at 300 and 350 Hz.

$$\frac{i_h^*}{i_h} = \frac{K_P s^2 + 2\zeta\omega K_P s + \omega^2 K_P}{Ls^3 + (2\zeta\omega L + R)s^2 + (\omega^2 L + 2\zeta\omega(K_P + R))s + \omega^2 R} \quad (20)$$

$$\left.\frac{i_h^*}{i_h}\right|_{\omega=\omega_h} = \frac{j2\zeta\omega_h^2 K_P}{j2\zeta\omega_h^2 (K_P + j\omega_h L + R)} = \frac{K_P}{K_P + j\omega_h L + R} \approx 1. \quad (21)$$

Fig. 8(b) shows the Bode plot for this control loop. With an injected signal frequency of 300 Hz, the gain was 0 dB and the phase delay was set to 0°.

Fig. 9 shows the regulation performance of the high-frequency current control at 300 and 350 Hz. The gain of the proportional regulator was set to ten times the impedance of the inductance. Despite the abrupt change in the frequency of the injected signal, the actual current signal followed the reference within one cycle of the injected frequency.

E. Control System Configuration

Fig. 10 illustrates the speed control system including the proposed tracking method. The fundamental speed control and current control loop were designed in the same manner as a conventional one described in [22]. The output of the speed control loop is the magnitude of the current reference vector and the angle of the current reference vector is determined by the θ control loop shown in Fig. 11. The integral regulator in Fig. 11 nullifies the MTPA criterion value P_o. The current references including the high-frequency injected signal are derived from the current reference block in Fig. 10 according to (7) and (8). After that, the current control block, which consists of the fundamental control loop and the supplementary control loop, generates the output voltage references.

IV. Experimental Results

To verify the feasibility of the proposed MTPA tracking method, an 11 kW IPMSM was pretested at 900 and 1750 r/min, and at different load torque conditions from 5 to 45 N·m in 5-N·m increments. The nominal parameters of the IPMSM under test are presented in Table I. At each torque and speed, the

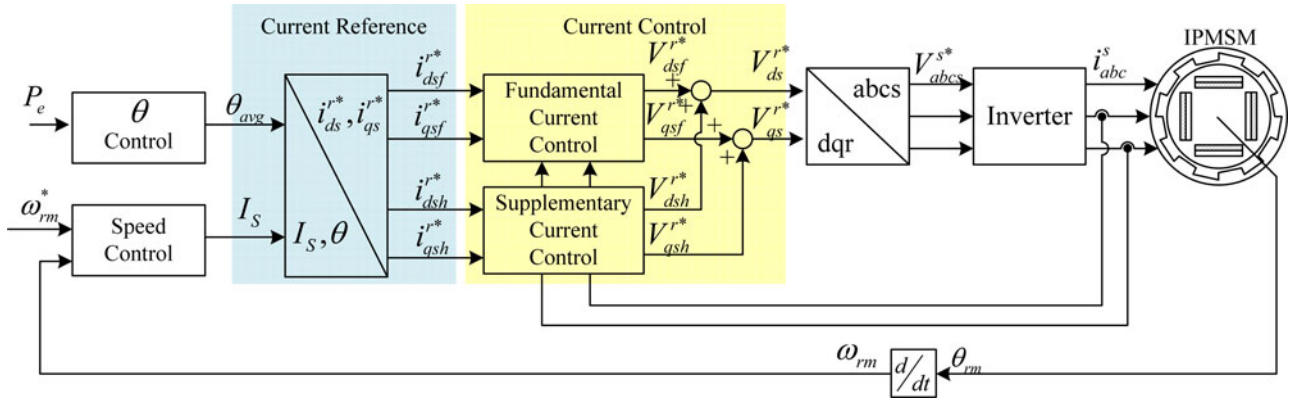

Fig. 10. Control system configuration.

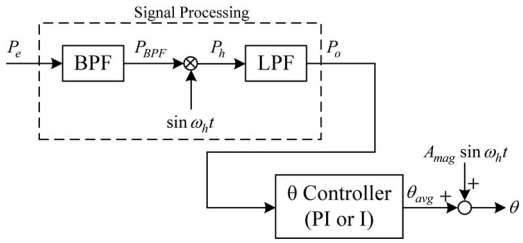

Fig. 11. Control block diagram for the current reference angle θ.

TABLE I
PARAMETERS OF THE IPMSM

Rated Power	11 kW
Rated Speed	1750 r/min
Rated current	39.5 Arms
Stator Resistance	0.14 Ω
Nominal Inductance	L_{ds}: 3.4 mH / L_{qs}: 4.3 mH
PM Flux linkage	λ_f: 0.253 V·s

magnitude of the stator current was recorded with the various current reference angles θ in order to find the MTPA operating point manually. After these pretests, the proposed MTPA tracking method was engaged to the drive system at each operating condition to compare the MTPA operating points from the proposed signal injection method with the MTPA operating points from the pretests. Fig. 12 shows the results of the comparison in which the MTPA operating points from the proposed method matched quite well with those from the pretests.

To clearly demonstrate the autonomous tracking capability of the proposed method, the current angle was manually adjusted from 0.5 to 0.6π rad and back to 0.5 π rad at 1700 r/min. After that, the proposed method was engaged at the same speed at two different load torques, 20 and 35 N·m, respectively. The results are shown in Figs. 13 and 14, respectively. In Fig. 13, the high-frequency current signal was injected for 10 s and the MTPA operating point was tracked. When the speed reached 1700 r/min and the load torque was 20 N·m, the current angle of the manual MTPA operating point was 1.78 rad and the tracked MTPA current angle was 1.82 rad. The difference in the current magnitudes was less than 0.05 A, which was less than 0.4% of

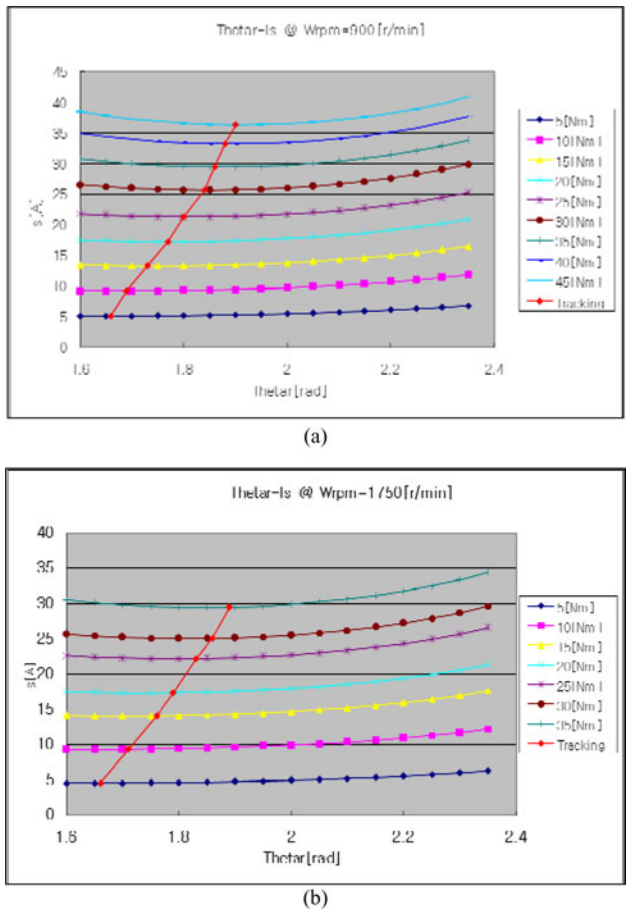

Fig. 12. Current magnitudes according to the current angle in the condition of specific load torque. The MTPA tracking results from the proposed method was also presented. (a) 900 r/min. (b) 1750 r/min.

the stator current at an operating point of 18.8 A. In Fig. 14, which is the case for the 35-N·m load torque, the MTPA current angle for the manual operation and proposed method was 1.85 and 1.89 rad, respectively. At this time, the difference in the current magnitude between the manual operation and the proposed method was less than 0.1 A, which is 0.3% of the magnitude of the stator current at that operating point.

In Fig. 15, the MTPA tracking performance of the proposed method is shown under conditions in which the load torque

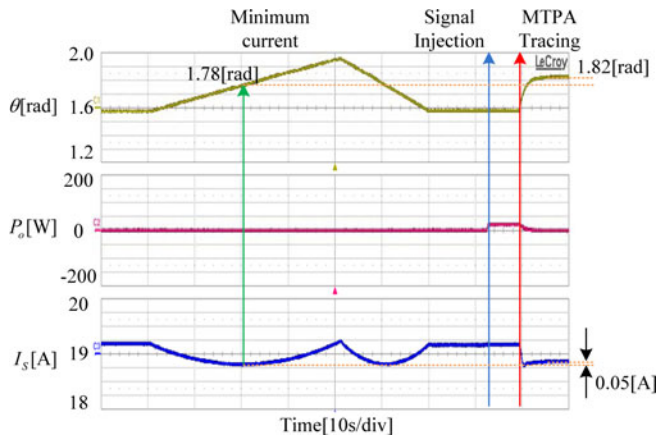

Fig. 13. Current angle, MTPA criterion value, and current magnitude at 1700 r/min and 20-N·m load torque.

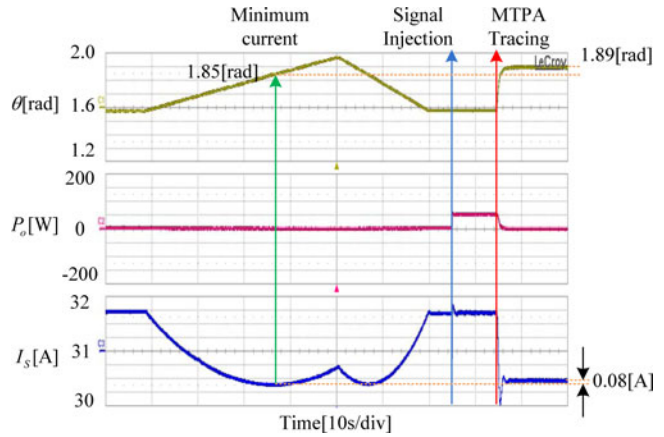

Fig. 14. Current angle, MTPA criterion value, and current magnitude at 1700 r/min and 35-N·m load torque.

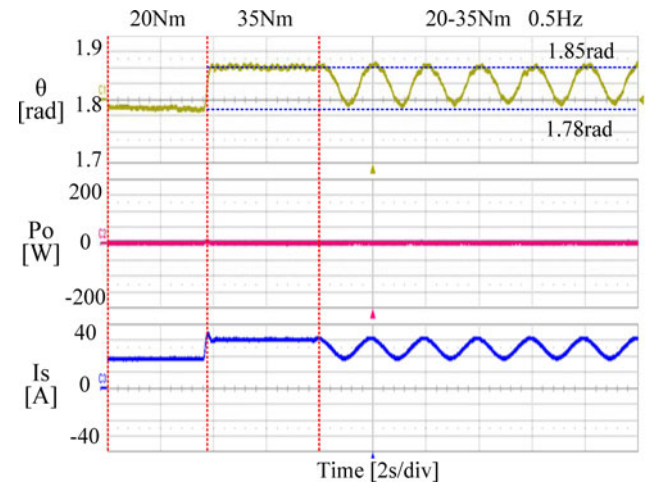

Fig. 15. Current angle, MTPA criterion value, and current magnitude at 900 r/min and load torque variation, 0.5 Hz, 20–35 N·m.

was varied. The IPMSM was controlled in the speed control mode at 900 r/min. At first, the load torque was 20 N·m and the proposed MTPA tracking method tracked the MTPA point as 1.78 rad, which was already confirmed in Fig. 12(a). Next, the load torque was increased to 35 N·m and the tracked MTPA point was 1.85 rad, which was also the MTPA point in Fig. 12(a). After that, the load torque varied from 20 to 35 N·m at a 0.5 Hz frequency. To regulate the speed of the IPMSM, the magnitude of the current was controlled by the speed control loop. Moreover, the proposed MTPA tracking method tracked the MTPA point instantaneously according to the current magnitude.

V. Conclusion

The proposed MTPA tracking method exploits the inherent characteristics of the MTPA operating point, in which the variation in the torque due to the variation in the current angle is zero at the MTPA point. This inherent characteristic of the MTPA operating point was analyzed with a machine model under the assumption of constant machine parameters and with a machine model that also considered the variation in the inductance. Injecting a small, high-frequency signal into the angle of the current reference vector, the variation in the torque was detected through the instantaneous input power of the IPMSM. The differentiation of the torque in terms of the angle of the stator current vector in the synchronous reference frame was calculated through signal processing of the input power. As shown in the experimental results, this proposed method tracked the MTPA operating point of the IPMSM without any premade lookup tables, machine parameters, and parameter estimation methods. The tracking error bound of the result was less than 0.5% in terms of the magnitude of the current.

Appendix

MTPA Condition That Considers the Variation in the Inductance

Under the assumption of constant machine parameters, the MTPA operating condition can be described as in (3). In addition, in the previous section, the MTPA tracking method was proven mathematically on the supposition that the inductances L_{ds} and L_{qs} are unknown, but constant. From now on, we will show that the proposed MTPA tracking method is applicable to cases in which the inductance varies according to the operating conditions.

In (A1), the torque equation is expressed with the current magnitude I_S and the current phase angle θ. To consider the variation in the inductances, the variations in inductances are regarded as

$$T_e = \frac{3P}{4}\left\{\lambda_f I_S \sin\theta + (L_{ds} - L_{qs})\, I_S^2 \frac{1}{2}\sin 2\theta\right\} \tag{A1}$$

$$L_{ds}(I_s,\theta)|_{I_s=\text{const}} \approx L_{ds}(\theta_{\text{avg}}) + \frac{\partial L_{ds}(\theta_{\text{avg}})}{\partial\theta}(\theta - \theta_{\text{avg}}) \tag{A2}$$

$$L_{qs}(I_s,\theta)|_{I_s=\text{const}} \approx L_{qs}(\theta_{\text{avg}}) + \frac{\partial L_{qs}(\theta_{\text{avg}})}{\partial\theta}(\theta - \theta_{\text{avg}})\,. \tag{A3}$$

At the MTPA operating point, the differentiation of the torque with respect to the angle of the current vector in the synchronous reference frame $\partial T_e/\partial\theta$ should be zero. Therefore, the MTPA condition can be derived as (A4). In comparison with that of constant inductance, the terms for the inductance variation according to the current angle θ were added in (A4), which represents the MTPA criterion taking into consideration the variation in the inductances

$$\frac{\partial T_e}{\partial\theta} = \frac{3P}{4} I_s \Bigg\{ \lambda_f \cos\theta + (L_{ds} - L_{qs})\, I_s \cos 2\theta + \left(\frac{\partial L_{ds}}{\partial\theta} - \frac{\partial L_{qs}}{\partial\theta} \right) I_s \frac{1}{2} \sin 2\theta \Bigg\} = 0. \quad \text{(A4)}$$

To get a signal corresponding to (A4), the calculated input power can be used under the assumption that the variation in the torque is very small and fast, and the variation in the speed, due to the injected signal, is filtered out by the system inertia. The injected current signals are the same with those in the previous section as in (A5). Due to the signal from the injected current, the *d*-/*q*-axis inductances L_{ds} and L_{qs}, derived from (A2) and (A3), can be expressed as

$$\theta = \theta_{\text{avg}} + \theta_h = \theta_{\text{avg}} + A_{\text{mag}} \sin\omega_h t \quad \text{(A5)}$$

$$L_{ds}(\theta) \approx L_{ds}(\theta_{\text{avg}}) + \frac{\partial L_{ds}(\theta_{\text{avg}})}{\partial\theta} A_{\text{mag}} \sin\omega_h t \quad \text{(A6)}$$

$$L_{qs}(\theta) \approx L_{qs}(\theta_{\text{avg}}) + \frac{\partial L_{qs}(\theta_{\text{avg}})}{\partial\theta} A_{\text{mag}} \sin\omega_h t. \quad \text{(A7)}$$

Then, the input power can be calculated from the general power equation (A8) and the voltage equation of the IPMSM (1). The input power consists of three terms: the copper loss, the reactive power due to the inductance of the IPMSM, and the mechanical power

$$P_e = \frac{3}{2}\left(v_{ds}^r i_{ds}^r + v_{qs}^r i_{qs}^r\right) = P_{\text{copper}} + P_{\text{reactive}} + P_{\text{mech}} \quad \text{(A8)}$$

$$P_{\text{copper}} = R_s I_s^2 \quad \text{(A9)}$$

$$P_{\text{reactive}}|_{\omega_h} = -\frac{1}{2} I_s^2 A_{\text{mag}} \omega_h \times \Bigg\{ (L_{ds}(\theta_{\text{avg}}) - L_{qs}(\theta_{\text{avg}})) \sin 2\theta_{\text{avg}} + \frac{1}{2}\left(\frac{\partial L_{ds}(\theta_{\text{avg}})}{\partial\theta} - \frac{\partial L_{qs}(\theta_{\text{avg}})}{\partial\theta} \right) \times A_{\text{mag}}^2 \cos 2\theta_{\text{avg}} \Bigg\} \cos\omega_h t \quad \text{(A10)}$$

$$P_{\text{mech}}|_{\omega_h} = \omega_r I_s A_{\text{mag}} \Bigg\{ \lambda_f \cos\theta_{\text{avg}} + \left(\frac{\partial L_{ds}(\theta_{\text{avg}})}{\partial\theta} - \frac{\partial L_{qs}(\theta_{\text{avg}})}{\partial\theta} \right) I_s \frac{1}{2} \sin 2\theta_{\text{avg}} + (L_{ds}(\theta_{\text{avg}}) - L_{qs}(\theta_{\text{avg}})) I_s \cos 2\theta_{\text{avg}} \Bigg\} \sin\omega_h t. \quad \text{(A11)}$$

The injected signal causes no variation in the current magnitude, but causes the variation in the current angle in the synchronous reference frame. Thus, copper loss due to the stator resistance is not affected by the injected signal as in (A9). However, the injected signal affects the reactive power and the mechanical power. The reactive power due to the injected signal can be summarized as (A10). To get the torque information from the input electric power, the injected frequency component of the reactive power should be separated from the input electric power. As in (A10), the reactive power is orthogonal to the injected signal. Additionally, the variation in the reactive power due to the injected signal can be filtered out with the proposed signal processing.

The mechanical power can be calculated as (A11). The mechanical power of the injected signal component is in phase with the injected signal. As a result, the output of the proposed signal processing, which is proportional to the MTPA criterion in (A4), can be derived as

$$P_o = \frac{1}{2} A_{\text{mag}} \omega_r I_s \Bigg\{ \lambda_f \cos\theta_{\text{avg}} + (L_{ds}(\theta_{\text{avg}}) - L_{qs}(\theta_{\text{avg}})) I_s \cos 2\theta_{\text{avg}} + \left(\frac{\partial L_{ds}(\theta_{\text{avg}})}{\partial\theta} - \frac{\partial L_{qs}(\theta_{\text{avg}})}{\partial\theta} \right) I_s \frac{1}{2} \sin 2\theta_{\text{avg}} \Bigg\}. \quad \text{(A12)}$$

Therefore, the proposed method based on signal injection can track the MTPA point even though the *d*-/*q*-axis inductances vary conspicuously.

REFERENCES

[1] N. Bianchi and T. M. Jahns, *Design, Analysis, and Control of Interior PM Synchronous Machines* (Tutorial course notes of IAS2004). Padova, Italy: CLEUP Univ. Press, 2004.

[2] J. M. Kim and S. K. Sul, "Speed control of interior permanent magnet synchronous motor drive for the flux weakening operation," *IEEE Trans. Ind. Appl.*, vol. 33, no. 1, pp. 43–48, Jan./Feb. 1997.

[3] T. M. Jahns, G. B. Kliman, and T. W. Neumann, "Interior permanent-magnet synchronous motors for adjustable-speed drives," *IEEE Trans. Ind. Appl.*, vol. IA-22, no. 4, pp. 738–747, Jul./Aug. 1986.

[4] S. Morimoto, K. Hatanaka, Y. Tong, Y. Takeda, and T. Hirasa, "High performance servo drive system of salient pole permanent magnet synchronous motor," in *Proc. IEEE Ind. Appl. Soc. Annu. Meet.*, 1991, pp. 463–468.

[5] B. Sneyers, D. W. Novotny, and T. A. Lipo, "Field weakening in buried permanent magnet AC motor drives," *IEEE Trans. Ind. Appl.*, vol. IA-21, no. 2, pp. 398–407, Mar./Apr. 1985.

[6] H. B. Kim, J. Hartwig, and R. D. Lorenz, "Using on-line parameter estimation to improve efficiency of IPM machine drives," in *Proc. IEEE Power. Electron. Spec. Conf.*, 2002, pp. 815–820.

[7] P. Niazi, H. A. Toliyat, and A. Goodarzi, "Robust maximum torque per ampere (MTPA) control of PM-assisted SynRM for traction application," *IEEE Trans. Veh. Technol.*, vol. 56, no. 4, pp. 1538–1545, Jul. 2007.

[8] Y. Jeong, S. K. Sul, S. Hiti, and K. M. Rahman, "Online minimum-copper-loss control of an interior permanent-magnet synchronous machine for automotive applications," *IEEE Trans. Ind. Appl.*, vol. 42, no. 5, pp. 1222–1229, Sep./Oct. 2006.

[9] Y. I. Mohamed and T. K. Lee, "Adaptive self-tuning MTPA vector controller for IPMSM drive system," *IEEE Trans. Energy Convers.*, vol. 21, no. 3, pp. 636–644, Sep. 2006.

[10] G. Kang, J. Lim, K. Nam, H. B Ihm, and H. G. Kim, "A MTPA control scheme for an IPM synchronous motor considering magnet flux variation caused by temperature," in *Proc. IEEE Appl. Power Electron. Conf. Expo.*, 2004, pp. 1617–1621.

[11] Y. S. Kim and S. K. Sul, "Torque control strategy of an IPMSM considering the flux variation of the permanent magnet," in *Proc. IEEE 42nd Ind. Appl. Soc. Annu. Meet.*, 2007, pp. 1301–1307.
[12] S. Morimoto, M. Sanada, and Y. Takeda, "Effects and compensation of magnetic saturation in flux-weakening controlled permanent magnet synchronous motor drives," *IEEE Trans. Ind. Appl.*, vol. 30, no. 6, pp. 1632–1637, Dec. 1994.
[13] C. Mademlis and V. G. Agelidis, "On considering magnetic saturation with maximum torque to current control in interior permanent magnet synchronous motor drives," *IEEE Trans. Energy Convers.*, vol. 16, no. 3, pp. 246–252, Sep. 2001.
[14] A. Consoli, G. Scarcella, G. Scelba, and A. Testa, "Steady-state and transient operation of IPMSMs under maximum-torque-per-ampere control," *IEEE Trans. Ind. Appl.*, vol. 46, no. 1, pp. 121–129, Jan./Feb. 2010.
[15] Z. Q. Zhu, Y. S. Chen, and D. Howe, "Online optimal flux-weakening control of permanent-magnet brushless AC drives," *IEEE Trans. Ind. Appl.*, vol. 36, no. 6, pp. 1661–1668, Nov./Dec. 2000.
[16] A. Dianov, Y.-K. Kim, S.-J. Lee, and S.-T. Lee, "Robust self-tuning MTPA algorithm for IPMSM drives," in *Proc. 34th Annu. Conf. IEEE Ind. Electron.*, 2008, pp. 1355–1360.
[17] S. Bolognani, L. Sgarbossa, and M. Zordan, "Self-tuning of MTPA current vector generation scheme in IPM synchronous motor drives," in *Proc. Eur. Conf. Power Electron. Appl.*, 2007, pp. 1–10.
[18] S. Bolognani, R. Petrella, A. Prearo, and L. Sgarbossa, "Automatic tracking of MTPA trajectory in IPM motor drives based on AC current injection," in *Proc. IEEE Energy Convers. Congr. Expo.*, 2009, pp. 2340–2346.
[19] S. Bolognani, L. Peretti, and M. Zigliotto, "Online MTPA control strategy for DTC synchronous-reluctance-motor drives," *IEEE Trans. Power Electron.*, vol. 26, no. 1, pp. 20–28, Jan. 2011.
[20] S. Kim, Y. D. Yoon, S. K. Sul, K. Ide, and K. Tomita, "Parameter independent maximum torque per ampere (MTPA) control of IPM machine based on signal injection," in *Proc. 25th IEEE Appl. Power Electron. Conf. Expo.*, 2010, pp. 103–108.
[21] S. Kim and S.-K. Sul, "Maximum torque per ampere control of interior permanent magnet synchronous motor based on signal injection," *Trans. Korea Institute Power Electron.*, vol. 15, no. 2, pp. 142–149, Apr. 2010.
[22] S. Morimoto, Y. Takeda, and T. Hirasa, "Current phase control methods for permanent magnet synchronous motors," *IEEE Trans. Power Electron.*, vol. 5, no. 2, pp. 133–139, Apr. 1990.

Sungmin Kim (S'09) was born in Seoul, Korea in 1980. He received the B.S. and M.S. degrees in electrical engineering from Seoul National University, Seoul, Korea, in 2002 and 2008, respectively, where he is currently working toward the Ph.D. degree.

His current research interests include power-electronic control of electric machines, sensorless drives, matrix converter drive, and power conversion circuits.

Young-Doo Yoon (S'06–M'10) was born in Korea. He received the B.S., M.S., and Ph.D. degrees in electrical engineering from Seoul National University, Seoul, Korea, in 2002, 2005, and 2010, respectively.

Since 2010, he has been with Samsung Electronics, Suwon, Korea. His current research interests include power-electronic control of electric machines, matrix converter drive, ultraprecision motion control, and electric home appliances.

Seung-Ki Sul (S'78–M'80–SM'98–F'00) was born in Korea in 1958. He received the B.S., M.S., and Ph.D. degrees in electrical engineering from Seoul National University, Seoul, Korea, in 1980, 1983, and 1986, respectively.

From 1986 to 1988, he was an Associate Researcher in the Department of Electrical and Computer Engineering, University of Wisconsin, Madison. From 1988 to 1990, he was a Principal Research Engineer with Gold-Star Industrial Systems Company. Since 1991, he has been a faculty member in the School of Electrical Engineering, Seoul National University, where he is currently a Professor. From 2005 to 2007, he was the Vice Dean of the College of Engineering, Seoul National University. From 2008 to 2011, he was President of the Korea Electrical Engineering & Science Research Institute. His current research interests include power-electronic control of electric machines, electric/hybrid vehicle drives, and power-converter circuits.

Kozo Ide (S'92–M'96) received the B.S., M.S., and Ph.D. degrees in electrical engineering from the Kyushu Institute of Technology, Kitakyushu, Japan, in 1991, 1993, and 1996, respectively.

From 1991 to 1992, he was a Visiting Researcher at L'Aquila University, Italy, supported by the Italian government. In 1996, he joined Yaskawa Electric Corporation, Kitakyushu, Japan, where he is currently a Manager of the R&D of Power Electronics. From 2002 to July 2003, he was a Visiting Researcher with Siemens AG, Germany. His current research interests include control technology for ac machines and energy conversion systems.

Dr. Ide is a member of the Institute of Electrical Engineers of Japan.